Mapping Surface Geochemical Data with GIS in Lower Lisbon Valley, Utah

MORGAN, Tanner

Department of Geosciences, Fort Lewis College, Durango, CO 81301

Spring | 2019

Abstract

At the Lisbon Valley Mining Company (SE Utah), exploration for sedimentary-hosted copper deposits has used both conventional soil sampling and sampling of ant hills for surface geochemistry. Anthill prospecting is a sampling technique that exploits the ants' natural sorting ability as they transport material from the subsurface. The data sets for each of these techniques can be compared using Geographic Information Systems (GIS) to evaluate the effectiveness of each sampling technique. Surface geochemistry is a commonly used tool in the exploration for ore deposits. GIS is a useful program for visualizing spatial datasets, such as soil geochemistry, fluid geochemistry, stratigraphy, and fault locations. Exploration using GIS provides a preliminary assessment that can help find possible economic mineralization comparing different retrieval methods of soil data provided by the mining company.

The mine lies on the eastern portion of the Colorado Plateau region within the section overlying the Paradox Basin. Structurally, the mine sits in the collapsed flank of a salt anticline with ore trends following normal faults in the section above salt. Deeper faults likely provided conduits for copper-rich fluids derived from Pennsylvanian sediments. Current mining operations exploit hypogene chalcocite with lesser amounts of bornite and chalcopyrite in sandstones and conglomerates of the Cretaceous Burro Canyon Formation and Dakota Sandstone. In lower Lisbon Valley, economic mineralization thus shows both stratigraphic and structural control. The faulted flanks of the valley provide economic copper, and the faulted valley graben and wash plain provide footprints for fluid flow of copper ions through the system.

Exploration has started further southeast from the mine along the faulted margins of the valley. Soil and anthill samples in the exploration areas were analyzed by ICP-MS, and concentrations were plotted by editing symbology. Similarities between the anthill and soil samples were identified. All sampling techniques revealed higher concentrations of copper proximal to the major normal faults associated with salt-anticline collapse, and the extension of structural control. This was as expected observing the current mining trend within the valley. The high copper concentrations near faults are consistent with the hypothesis that faults controlled flow of fluids that made ore deposits possible. Spatial analyses maps based off conversion of bulk composition to point data illustrates prospects in Lower Lisbon Valley as viable options for economic extraction of copper.

Background – Geologic Setting

The mine and area of study is in Lower Lisbon Valley approximately 30 miles southeast of the La Sal Mountains, Utah (Fig. 1). The sediments in this area can host an assortment of potentially economic minerals. The main economic deposits are copper, but the mining district includes commercial mining of potash and uranium as well as natural gas production.

Having such a treasure trove of resources, the Lisbon Valley area can owe its wonderful deposits to its fractured sedimentary units. Lisbon Valley lies on the eastern portion of the Colorado Plateau region within the section overlying the Paradox Basin. These sediments have had an extensive history of fluid migration spanning multiple generations of petroleum movement and mineral growth.

The Paradox Basin is bounded on northeast and east by the Uncompahgre uplift segment of the Ancestral Rockies orogenic system and is surrounded along the remainder of its periphery by paleotectonically controlled shoals (Baars, 2003). The deepest part of the basin is directly adjacent to the uplift. These Pennsylvanian age sediments are a product of periodic basin filling and isolated marine circulation resulting in cyclical deposits of dolomite, gypsum, chloride and sulfate salts, and organic-rich fine clastics (Adkins et. al. 2011). Salt deposition began very early Desmoinesian (middle Pennsylvanian) time in the deeper faulted troughs (Hite, 1960) and slowly filled the structural basin, burying the basement faults by the end of the epoch. Most of the small structural features of the Paradox Basin were in place and growing during that time following the trend of Precambrian normal faulting. Over the ages the Paradox Formation was buried, and the faults moving syndepostionally with the newer units being deposited and lithified. The Colorado Plateau was subjected to subsidence, deposition, erosion, and in the late Cretaceous the compression of the Laramide Orogeny.
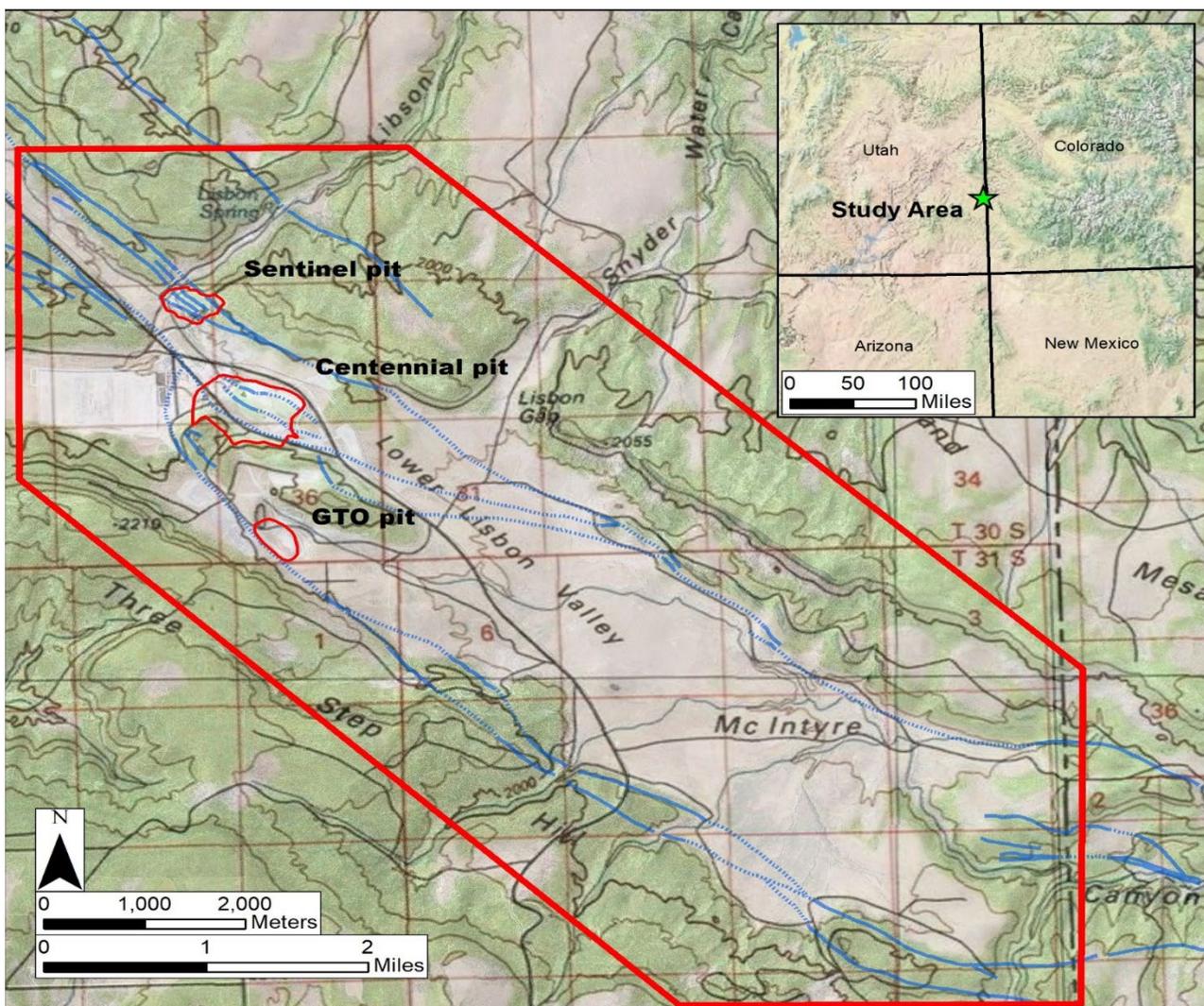

Figure 1 – Location Map of Lower Lisbon Valley, Utah (Blue lines indicate normal faults)

3

Salt Anticlines

The most prominent and most interesting structural features of the Paradox basin are the large, positive structures formed by salt flowage and diapirism in east-central Utah and west-central Colorado (Baar, 2003). This broad region, termed the "Paradox fold and fault belt" by Kelley (1955), overlies the deeper structural depression of the Paradox basin where depositional salt thickness may have reached 5000 to 8000 ft. These salt features can be seen today as faulted or collapsed diapirs. From these sedimentary features come economic mineralization along their faulted margins; the heavily fractured beds create excellent conduits for mineral-rich fluids to migrate.

Unit Description

The main rock units that bear economic mineral deposits within the valley are concentrated in the sandstones and conglomerates within the Burro Canyon Formation and Dakota Sandstone. This package of mineralized sediments is bounded from below by the Jurassic Morrison Formation and capped up above by Mancos Shale (Fig. 2).

Morrison Formation – Jurassic – (Jms)
Deposited in the late Jurassic, the Morrison Formation is composed of two members. The lower Salt Wash Member is a brown fluvial sandstone interbedded with red, brown mudstones and thinly bedded gray limestones; and the upper Brushy Basin Member consists of variegated bentonitic mudstones, and conglomeratic sandstones. Portions of the Morrison can contain uranium/vanadium deposits in some of the channel sandstones.

Burro Canyon Formation – Early Cretaceous – (Kbc)
These Early Cretaceous fluvial deposits overlie the Morrison. The lower half of the Burro Canyon has lenses of conglomeratic sandstones indicative of braided river systems, while the upper portion consists of variegated beds of green and purple mudstones interfingering with fluvial sands.

Dakota Formation - ~M. Cretaceous – (Kd)
The Dakota Formation is a package of fluvial conglomeratic sandstones interbedded with green, gray, and black mudstones. During the transgression of the Cretaceous sea, sedimentation of these fluvial deposits sits atop the Burro Canyon Formation. The Dakota Sandstones and Burro Canyon Formation are the host of copper deposits within the valley.

Mancos Shale – M-L. Cretaceous – (Kms)
The Mancos Shale sits unconformably over the Dakota Formation and is composed of thick gray fossiliferous shales. The Mancos Shale is the youngest of the Cretaceous units in Lisbon Valley, and prominently preserved in small fault wedges along the hanging wall.

Structures

The valley in which the mine is located can be interpreted as a collapsed salt anticline with normal faulting trending northwest-southeast. Copper occurrences occupy the northwest and southeast ends of the Lisbon Valley anticline. The displaced valley half-graben consists of heavily fractured Burro Canyon Formation and Dakota Sandstone.

Outcrops on the northeastern flank of Lisbon Valley show signs of bleached Burro Canyon and Dakota formation from hydrocarbon migration. On the southwest side, Jurassic rocks (Morrison Formation through Wingate Sandstone) dip gently off to the southwest. A complex trend of normal faults down-drops the crest of an underlying salt body so that Cretaceous Mancos Shale and Dakota Formation are exposed in a topographic valley (Adkins et. al. 2011). On the opposite side of the valley, Morrison, Burro Canyon, and Dakota Formations dip gently off to the northeast and are cut by a series of normal faults that appear to be largely antithetic to the faults on the southwest side.

Unit Names for Geologic Map Legends:

|		
Qea	: Mix eolian and alluvial	Ject : Entrada Fm, Slick Rock Member
Qms	: Slumps/Landslides	Jcd : Carmel Fm, Dewey Bridge Member
Km	: Mancos Shale	Jn : Navajo Fm
Kd	: Dakota Sandstone	Jk : Kayenta Fm
Kbc	: Burro Canyon Fm	Jw : Wingate Fm
Jmb	: Morrison Fm, Brushy Basin Mem.	TRc : Chinle Fm
Jms	: Morrison Fm, Salt Wash Mem.	IPhu : Paradox Fm, Upper Honaker Trail Mem.
Jmst	: Morrison Fm, Summerville Mem.	IPhl : Paradox Fm, Lower Honaker Trail Mem.
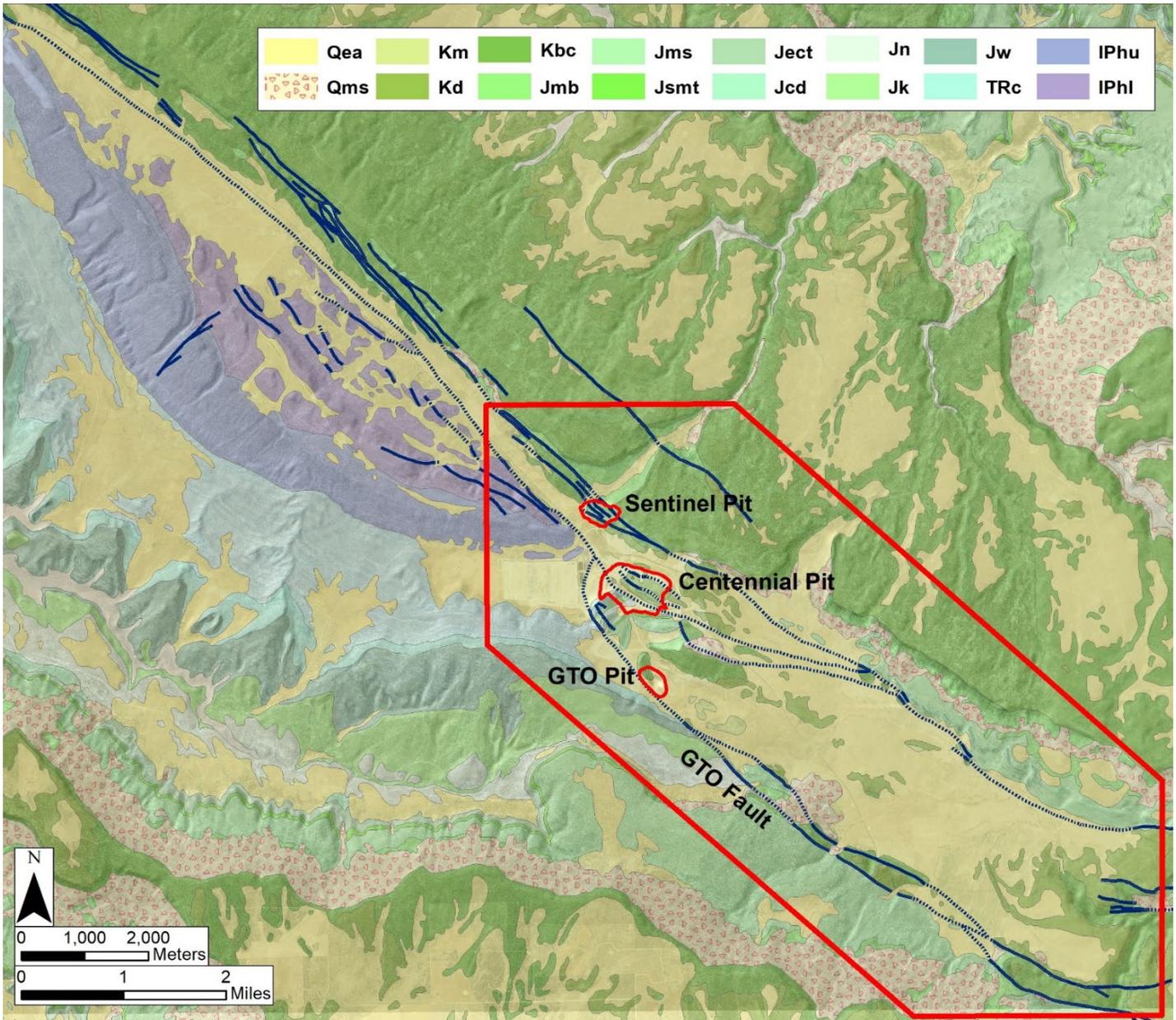
Figure 2 – Geologic Map of Lower Lisbon Valley, (Blue lines indicate normal faults).

Copper mineralization

The paleo-fluid history of Lisbon Valley is important for stratiform sediment-hosted copper (SSC) deposits (Robb, 2017), because these deposits are typically hosted in intracontinental, rift-related sedimentary sequences (i.e. the Paradox Basin). The early part of the sequence was either deposited originally as an oxidized (red bed), aeolian to evaporitic assemblage, or was rapidly oxidized during burial and diagenesis. This sequence is then overlain by sediments from a shallow marine transgression that deposited a more reduced assemblage of shales, carbonates, and evaporites.

The petroleum products, liquid petroleum, natural gas, sulfur, and bitumen are first controlled by distribution of petroleum source rocks, but most of their history is controlled by the aqueous fluids that were co-produced under petroleum-generation or petroleum-cracking conditions. The aqueous fluid co-produced during petroleum generation alters the rocks through which it flows, which is a critical rock-preparation step that controls the copper resources of the basin, and possibly controls the source of copper as well. The uranium and vanadium systems of the Basin appear to be controlled by circulation of basinal aqueous fluids and the reduction capacity of hydrocarbons and sour H_2S-rich natural gas (Fleshman, 2005). The chemistry of modern groundwater and formation waters in the Paradox Basin reflects that long fluid history of the Basin.

In Lower Lisbon Valley, small outcrops of copper mineralization and small prospects occur along the normal faults that flank both sides of the valley. There are two phases of alteration in the copper deposits found; pre-mineralization rock preparation, and alteration associated with the copper event. The primary hypogene copper mineral extracted from this area is chalcocite (Cu_2S), with lesser amounts of bornite (Cu_5FeS_4) and chalcopyrite ($CuFeS_2$) (Lantz Indergard, 2018, personal communication). The secondary copper mineralization occurs from alteration caused by meteoric waters in the supergene; disseminated amounts of azurite ($Cu_3(CO_3)_2(OH)_2$) and malachite ($Cu_2(CO_3)(OH)_2$) can be seen in outcrop sometimes covered in a weathering rind of cuprite (Cu_2O). Supergene chalcocite can be observed but to lesser amounts than the copper carbonates.

Sedimentary rocks along the Lisbon Valley fault zone have generally been bleached, and porous Burro Canyon Formation has been silicified for 50 or more feet away from the fault on the hanging-wall side. Solution activity in the fault zone is indicated by bleaching, silicification, and deposition of copper sulphides (Jacobs and Kerr, 1965). Weak or poorly defined zoning patterns between these sulfides and pyrite have been noted, and the pyritic halo around the copper has occasionally been found to contain anomalous amounts of lead or zinc (Adkins et al., 2011). The copper sulfide zoning conforms to the usual pattern in deposits of this type: most of the deposit is chalcocite, with increasing amounts of bornite near the margins, and a narrow rind of chalcopyrite + iron carbonate at the fringes of the copper zone.

Methods

This project is based on data provided by the Lisbon Valley Mining Company. The data consists of chemical analyses of samples collected during exploration for future copper mining. All samples were analyzed by a third-party lab using Inductively Coupled Plasma Mass Spectrometry (ICP-MS). ICP-MS is a highly-sensitive analytical technique that measures elemental concentrations. ICP-MS combines a high-temperature induced coupled plasma source with a mass spectrometer. The ICP source converts the atoms of the elements in the sample to ions. These ions are subsequently separated and detected by the mass spectrometer, solid sample concentrations are indicated in parts per million (ppm).

Most of the samples that were collected and analyzed came from Lower Lisbon Valley. The samples are divided into two varieties: surface samples collected along the flanks of the valley with prominent Burro Canyon exposure, and anthill samples collected throughout the wash plain of the valley. The anthill samples were collected using a technique called anthill prospecting, a process that exploits the ants' natural sorting ability as they transport material from the subsurface. The anthills used for sampling were approximately one to three meters in diameter and showed no signs of life (Fig. 3a). The anthills were selected at random intervals, exhumed, then dry sieved. Grain size was consistent throughout anthill, but some contained larger grain sizes

within the hill, so a distinction was made among them to see if grain size affected bulk mineral concentrations (Fig. 3b). The faulted flanks of the valley provide economic copper, and the faulted valley graben and wash plain provide footprints for fluid flow of copper ions through the system. The reasoning behind collecting anthill samples was to see the collection of these altered copper minerals as the copper ions move from the heavy concentrated flanks to the valley floor. Another reason was to see whether the ants have excavated down to the C-horizon, a zone of significance in the likelihood that this horizon can be indicative of copper in the underlying bedrock.

A hand sample was collected from the Centennial Pit waste pile for SEM analysis to assess the cement and grain chemistry within the zones of interest. Elemental sample spectra were created using the signatures given off by backscatter-electrons. Backscatter electrons (BSE) are electrons that have penetrated the sample surface and interacted with the elements in the subsurface of the thin section. They are helpful to determine chemical compositions of specific grains and can indicate/map relative atomic densities of afore mentioned grains for transition metals, nonmetals, metalloids, and/or rare earth metals. BSE are used to show spatial variations in chemical compositions; acquiring elemental maps or spot chemical analyses using Energy Dispersive Spectroscopy (EDS). This can help distinguish between phases based on mean atomic number (commonly related to relative atomic density) or used for rapid discrimination of phases in multiphase samples as X-ray images displaying spatial elemental concentration in the form of composition maps.

Figure 3a – Aerial image displaying approximate size of anthills along Lisbon Valley Rd, Utah
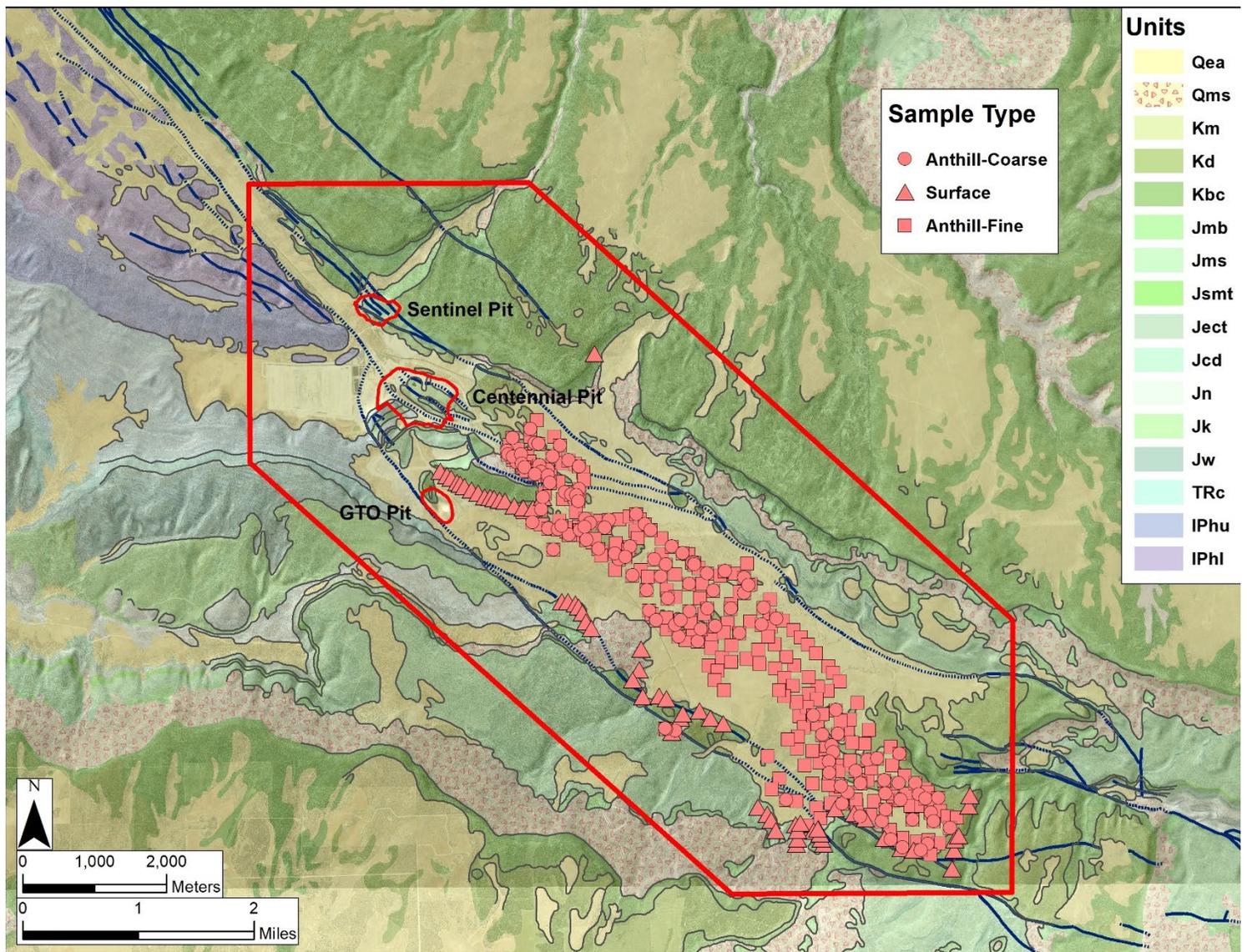
Figure 3b – Location map of anthill samples from the valley floor, and surface samples from the valley flanks.

Results

Surface geochemistry is a commonly used tool in the exploration for ore deposits. Exploration using GIS provides a preliminary assessment that can help find possible economic mineralization comparing different retrieval methods of soil data. The reason it is imperative to understand the paleo-fluid history of the valley is because the ore extraction technique the mines has proposed uses in-situ leach recovery. Also known as solution mining, this process uses boreholes to inject a weak acid into an economic deposit and slowly dissolve the metals into a mobile solution. The solution after some time will have enough metallic ions mobilized that the slurry can then be recovered. The porosity and permeability are controlled both by stratigraphic and structural controls. The study mainly focuses on geochemical signatures best for exploration but variable cementation in the rock record is also a factor when injecting fluids into strata.

SEM Analysis

A sample was collected from the Centennial Pit waste pile. The unit correlative to the sample from its texture, sorting, and features say it was likely Cretaceous Burro Canyon or Dakota Sandstone. Under the SEM, the sand grains are primarily quartz, with smaller amounts of K-feldspar, and the pore spaces contain several different cements. The cements in this sample include: (1) clay minerals; (2) gypsum; (3) barite (intergrown with clay minerals in some cases (Fig. 4a)); copper oxide (cuprite) or carbonate; and copper sulfide (chalcocite)

8

(Fig. 4a; Fig. 4b; Fig. 5; Fig. 6). The sample illustrated below has barite growth in the pore space between grains. Grains of altered feldspars along the copper cemented fracture zone were observed (Fig. 6) and areas around the cementation were points of interests for this study.
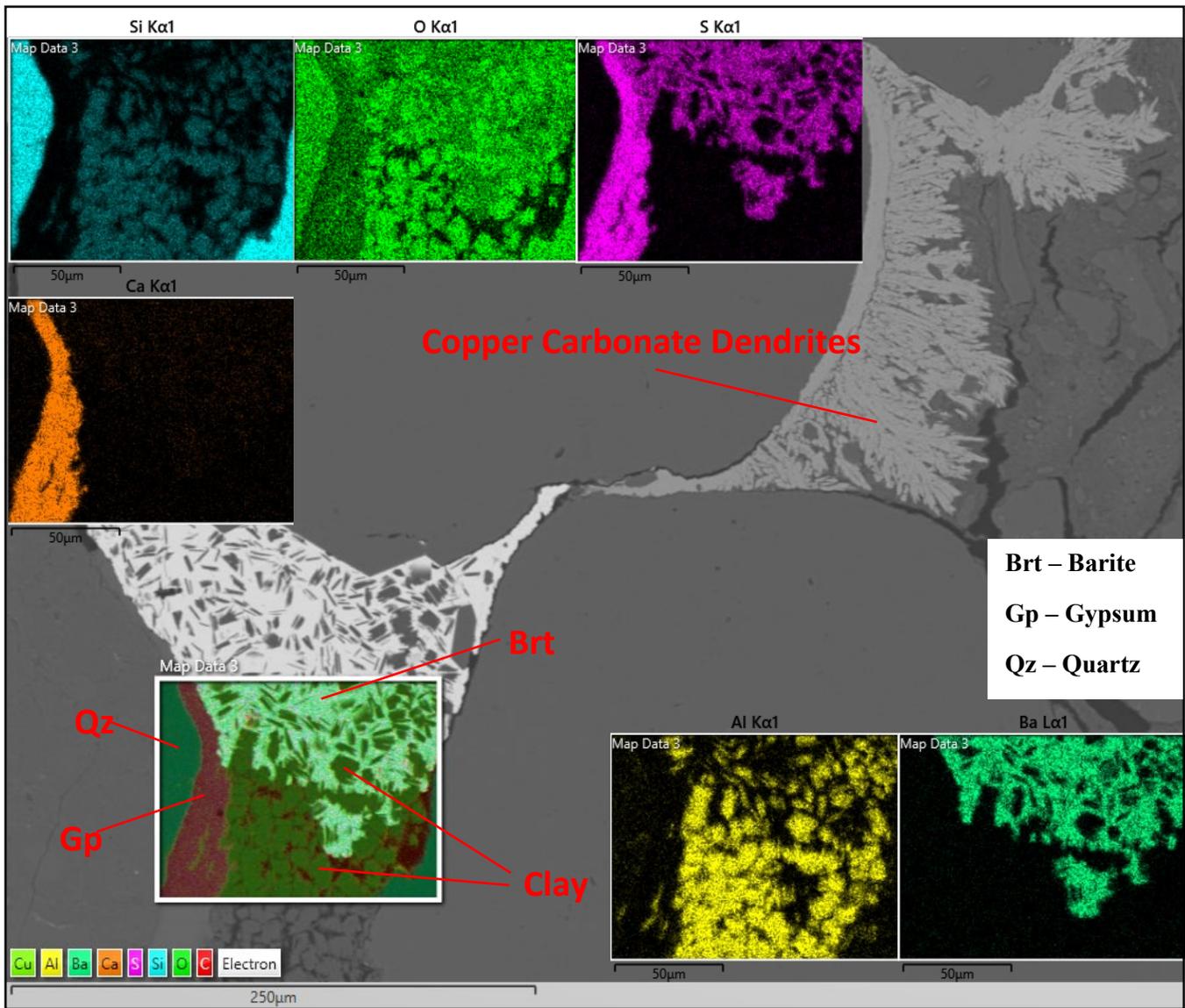

Figure 4a – SEM backscatter electron colored composition maps, barite cementation
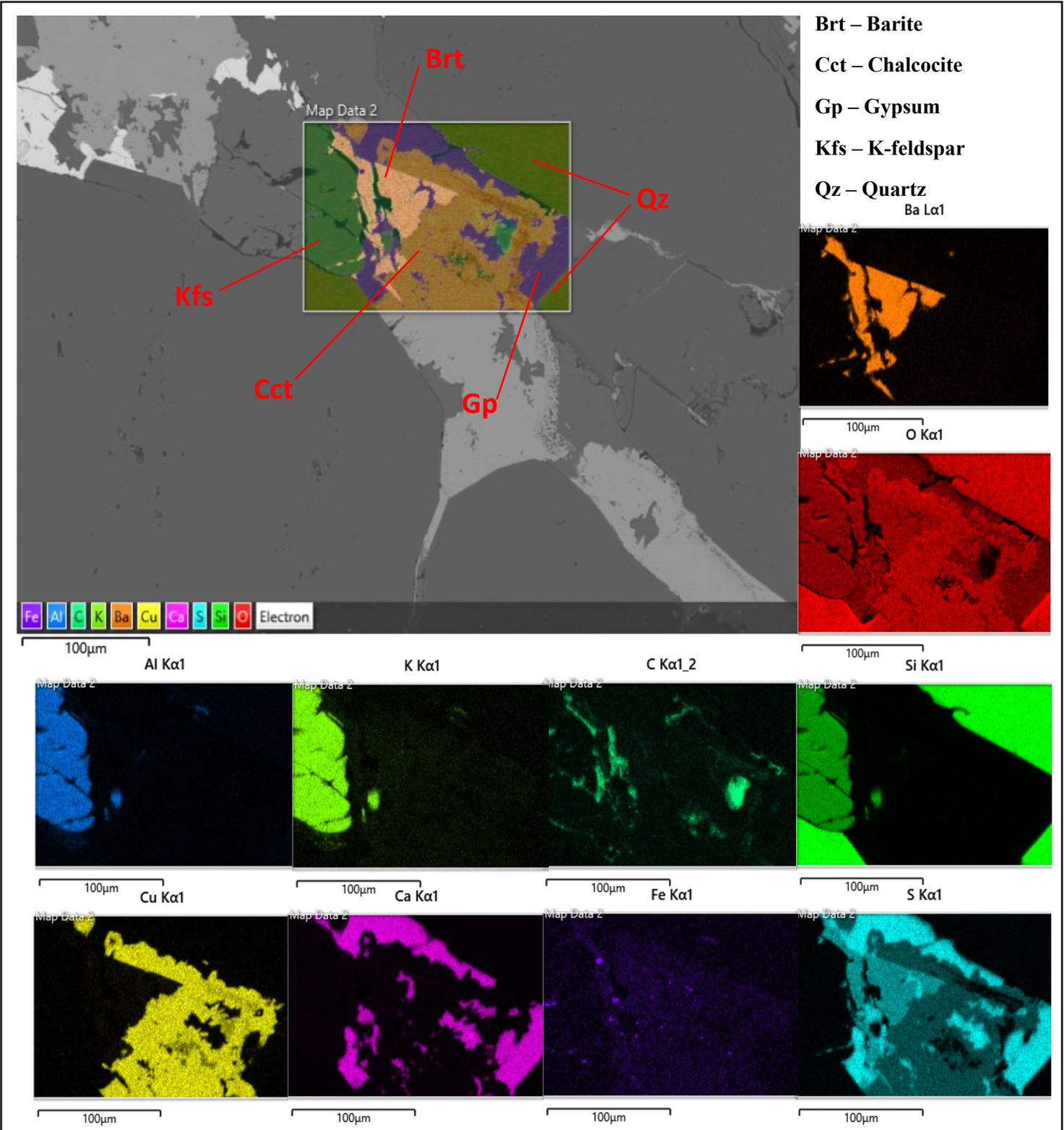
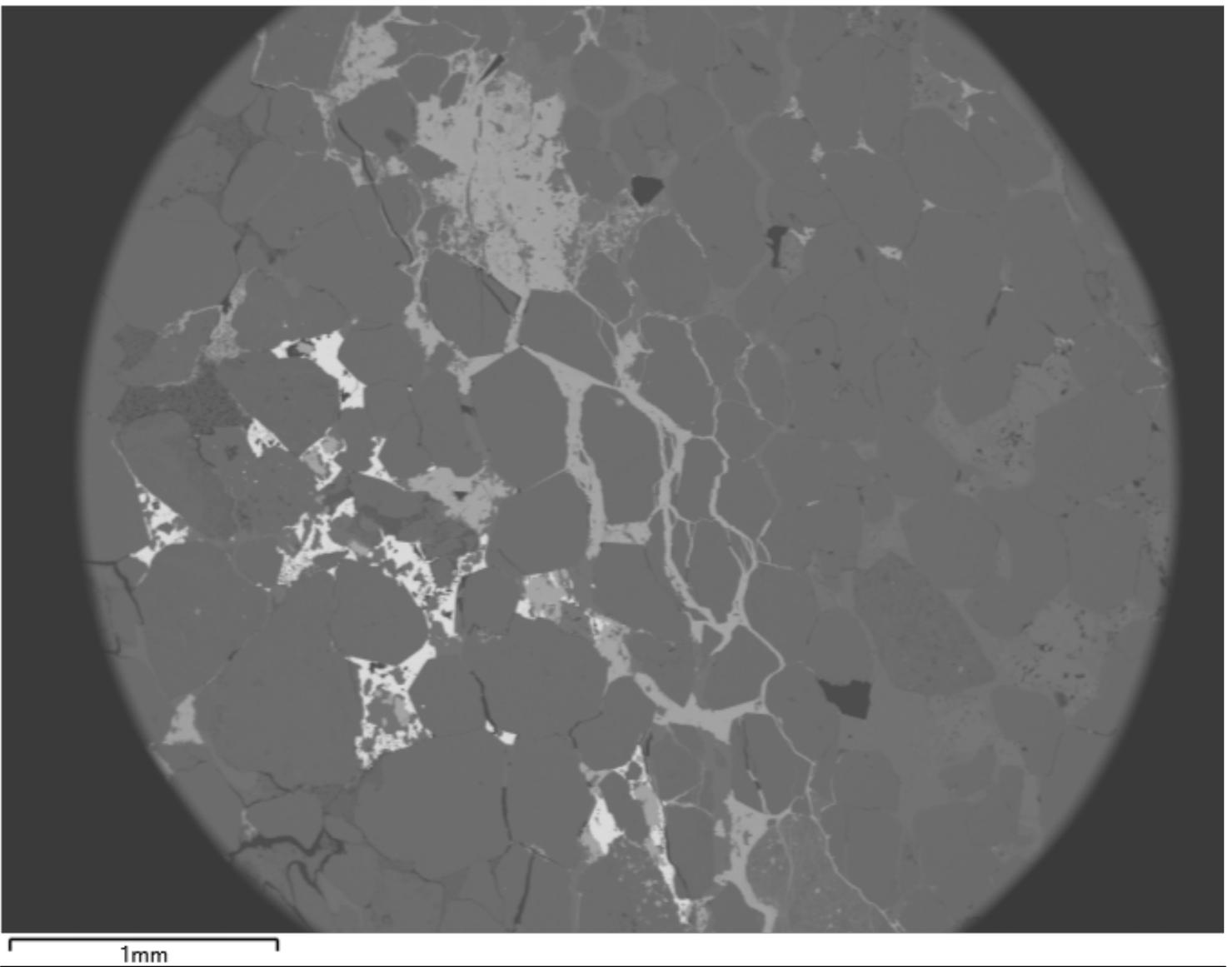Figure 4b – SEM backscatter electron colored composition maps, copper with barite cementation.

1mm

Figure 5 – Electron image taken from sample displaying barite and copper cements.

Section Summary

Instrument parameters with BSE affect the interaction volume (or beam penetration) which increases with increased acceleration voltage and decreases with increasing atomic number (heavier elements will show up brighter in grayscale). The image above has the brightest mineral as barite. The second brightest minerals contain copper (oxides, carbonates, and sulfides) and the lowest brightness represents cements such as quartz, clays, and gypsum. Changing beam current or lowering acceleration of voltage can affect the overall spectral resolution of the specimen. The size of the pixels will be larger/grainier when rastering in data and may skew results. The opposite might occur if the beam current and voltage acceleration is increased, the image may have a sharper resolution image, but might create a problem with irradiating the surface of sample.

Initial EDS analysis usually involves the generation of an X-ray spectrum from the entire scan area of the SEM. Next page (Fig. 6) is a secondary electron image of the sample from the Centennial pit waste pile and with its corresponding X-ray spectra that was generated from the entire scan area in (*Appendices 1- The Y-axis shows the counts (number of X-rays received and processed by the detector) and the X-axis shows the energy level of those counts in kiloelectron volts (keV))*. SEM analyses on clay filled pore spaces were unable to distinguish the types of clays, only indicate presence of phyllosilicates.
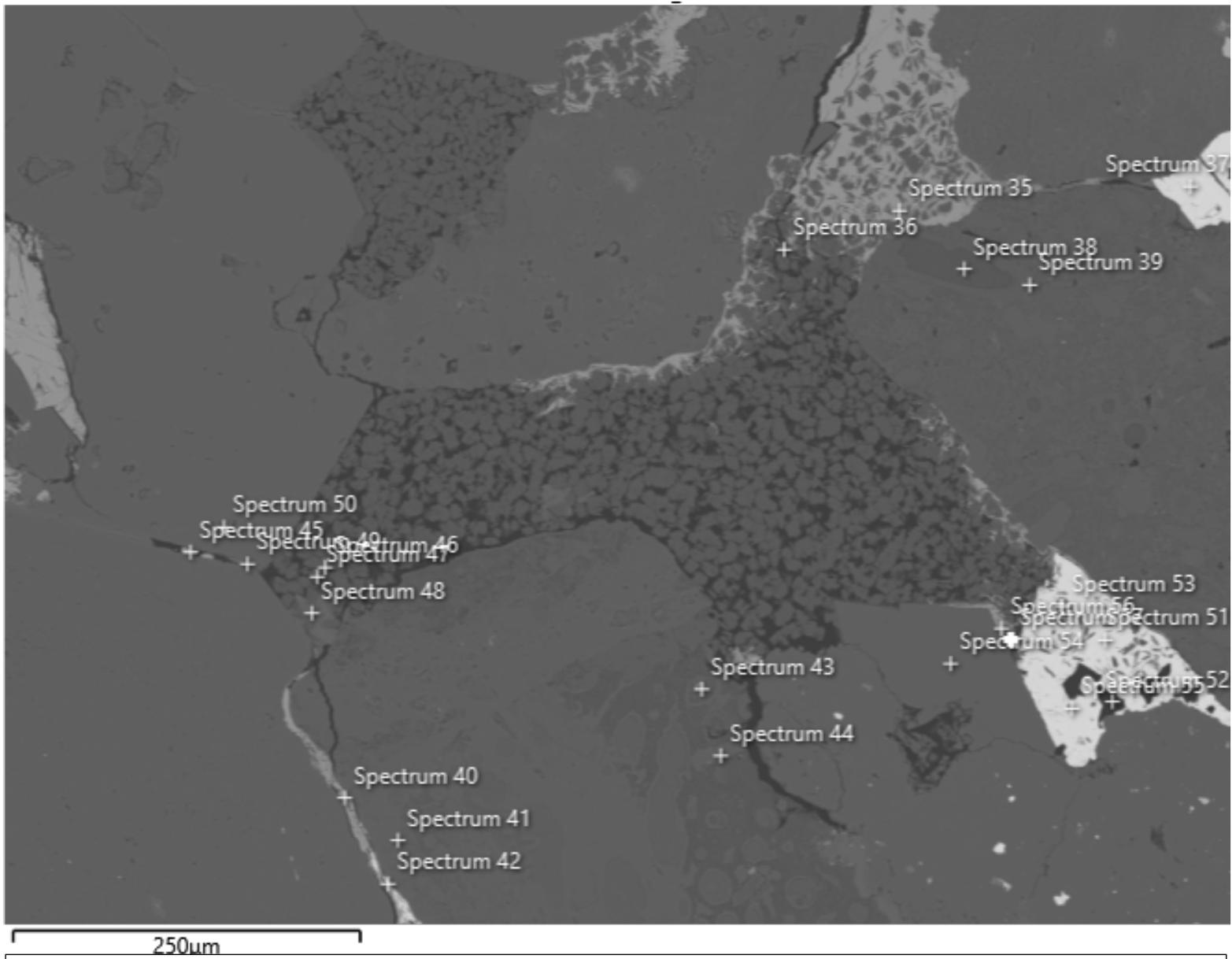
Figure 6 – Sample points with corresponding elemental spectra in (Appendices 1).

Spatial Analysis Summary

GIS has numerous spatial analyst tools used to spatially correlate or extrapolate feature classes such as points, poly-lines, polygons and non-feature classes like rasterized files. For this study I used bulk rock chemical data provided by the mine to assess where and what kind of elements are associated with copper mineralization. The associative minerals found with copper at the mine are chalcopyrite ($CuFeS_2$) and bornite (Cu_5FeS_4). The barite cements ($BaSO_4$) are part of a partial solid-solution series with anglesite ($PbSO_4$). All the minerals have certain metallic ratios that provide trends which can be mapped spatially over a georeferenced layer or framework (Fig. 7a; Fig. 7b). These trends are then correlated with proximity to faults and unit type to provide a model that could look at other element ratios like the difference between naturally occurring copper versus anthropogenic occurrences.

From the figures, copper concentrations are highest along the GTO Fault and other faults located in the middle of the valley. Highest concentrations of copper are within the Burro Canyon Formation, while fine anthill samples taken from Quaternary units had lower amounts of copper. The high ratios of copper to other elements correlate spatially with high copper concentrations.
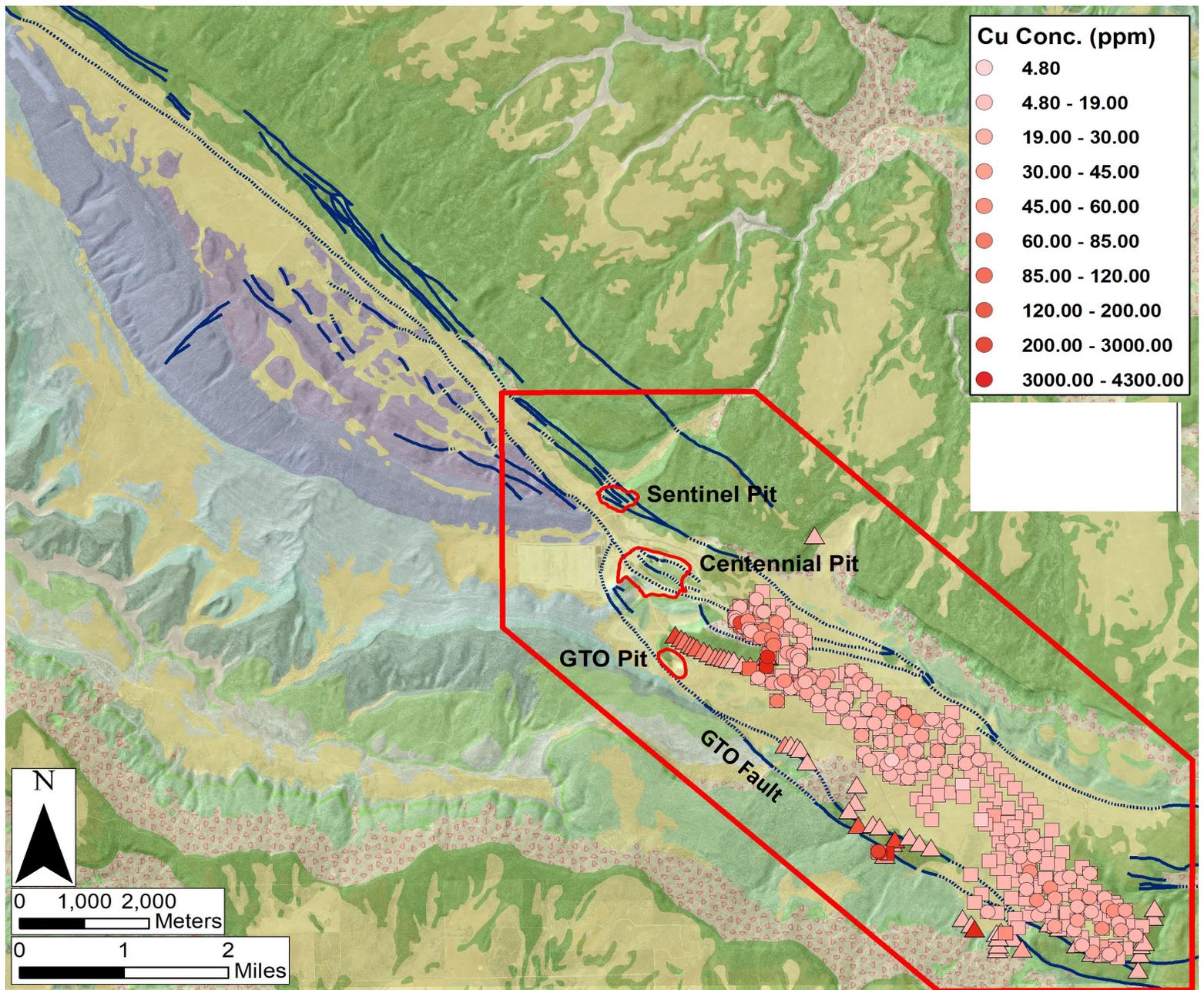
Cu Conc. (ppm)
- 4.80
- 4.80 - 19.00
- 19.00 - 30.00
- 30.00 - 45.00
- 45.00 - 60.00
- 60.00 - 85.00
- 85.00 - 120.00
- 120.00 - 200.00
- 200.00 - 3000.00
- 3000.00 - 4300.00

Sentinel Pit

Centennial Pit

GTO Pit

GTO Fault

N

0   1,000 2,000
Meters

0   1   2
Miles

Figure 7a – Sample locations showing spatial distribution of copper in Lisbon Valley

13
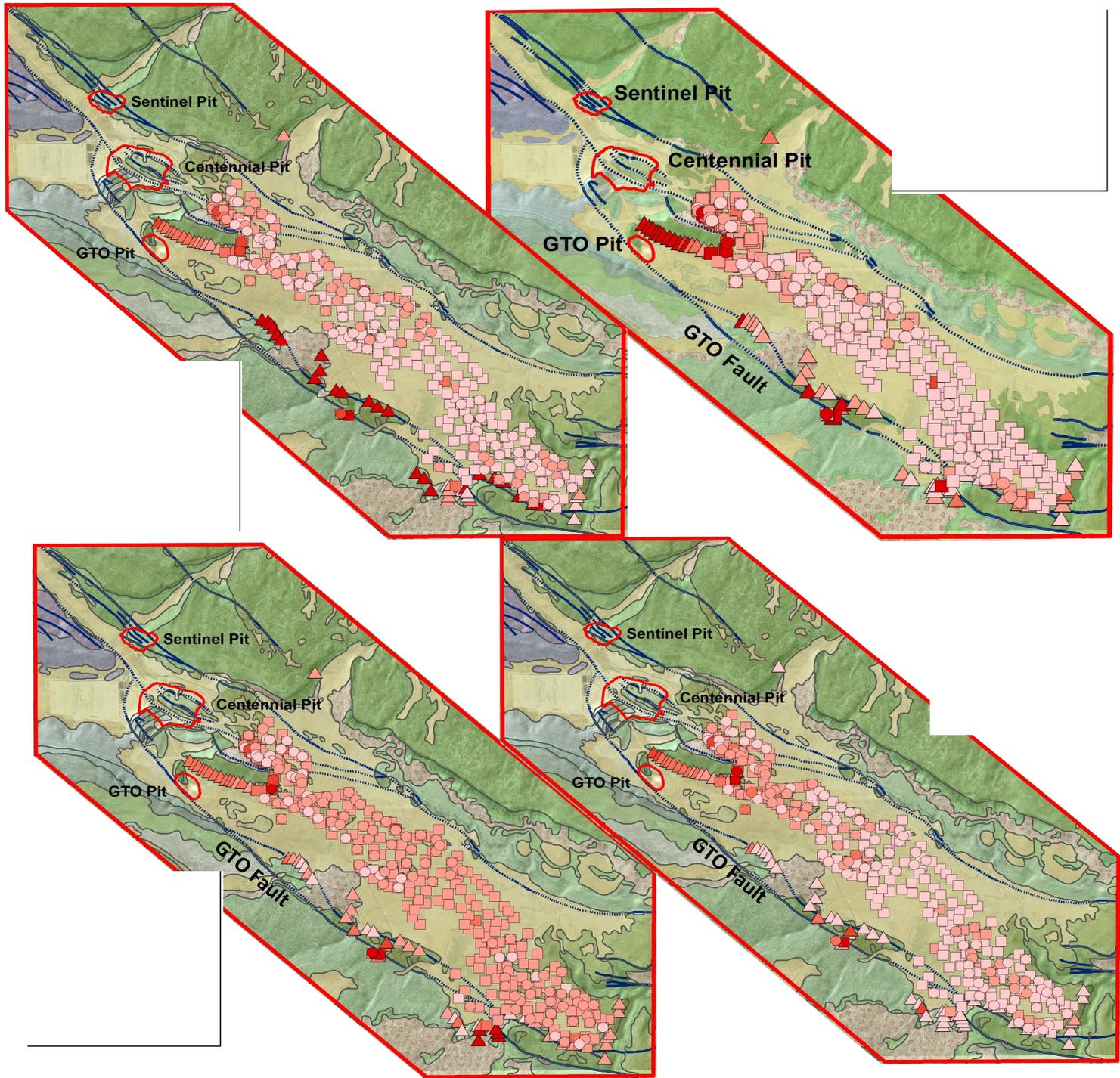
Figure 7b – Sample locations showing metal ratios compared to copper.

Discussion/ Conclusion

Exploration has started further southeast from the mine along the faulted margins of the valley. With the bulk composition ICP data, the concentrations were plotted using GIS. Sample proximity to faults was calculated to understand the degree of mineralization towards and away from the faulted flanks. Cross-plots depicting copper to associated elements were created to find relationships between the ore deposit and the connate fluids that carried copper ions before deposition (Fig. 8a; Fig. 8b; Fig. 8c; Fig. 8d). The copper

concentrations on all cross-plots are on a logarithmic scale in (ppm). All associative metals are on logarithmic scales in (ppm), except iron graphed as bulk percent due to its widespread presence in the valley.

Stratiform sediment-hosted copper deposits relate mainly to the types of sediments through which the fluids have traveled prior to deposition and also to the contrasting properties of Cu, Pb, Fe and Zn in the solutions (Robb, 2017). Chemically the basinal brines must have been channeled into oxidized (red bed) aquifers (i.e. Permian Cutler and Triassic Chinle Formations) and able to scavenge all three base metals from the fertile detritus in the basin, but the resulting ore fluid would be saturated only with respect to Cu and under saturations of Fe, Pb and Zn.

The reason we look at iron, lead and zinc saturations are because of the replacement textures in different sulphide mineral's paragenetic sequences and the transgressive nature of ore zones related to lithologies. The zones of mineralization in the valley represent a chemical front in the footwall of the ore zone and against which a zoned sequence of base metal sulphides (Chalcocite – bornite – chalcopyrite) is arranged.

The sample used for SEM analyses illustrated barite growth in the pore space between grains. This is important to note because understanding barite cementation provides background on how the paleo-fluids flowed as well as how the weak acid injection wells will overall affect the cemented rock once ions are mobile. A helpful characteristic behind the history of the barite cementation was during its migration and before it became stable, the paleo-solution had to have carried copper ions. If that is the case, then the barite cement should provide a footprint for the fracture-controlled dissemination of copper rich fluids as it migrated from its source to the hypogene and into the supergene.

The cross plots showed Cu/Fe, Cu/Zn, and Cu/Pb ratios having two different trends. The highest copper concentrations associated with low Fe and low Pb. Ratios for Cu/Ba had three different patterns, possibly because the copper signatures are from different copper minerals. High Cu/Fe ratios could indicate presence of chalcocite, and lower Cu/Fe trends could indicate presence of chalcopyrite or bornite. Spatially Cu/Pb and Cu/Ba are the locations of highest copper, although barite cement was found in the sample from the mine, high Ba does not correlate with highest copper concentrations. The highest copper concentrations were proximal to the normal faulting. This was as expected, observing the current mining trend within the valley. The high copper concentrations near faults are consistent with the hypothesis that faults controlled flow of fluids that made ore deposits possible.

Spatially surface and anthill samples provided similar information; the coarse anthill samples specifically shared similar values and trends to traditional surface samples. This means coarse anthill samples could potentially be an alternative technique to soil sampling. Fine anthill samples show lower concentrations of all metals, probably because the valley gets periodic sheet flows depositing fine grained sediments and frequent winds blowing in fine loess. This would be a reason why the fine anthill samples should not be an alternative to traditional sampling.
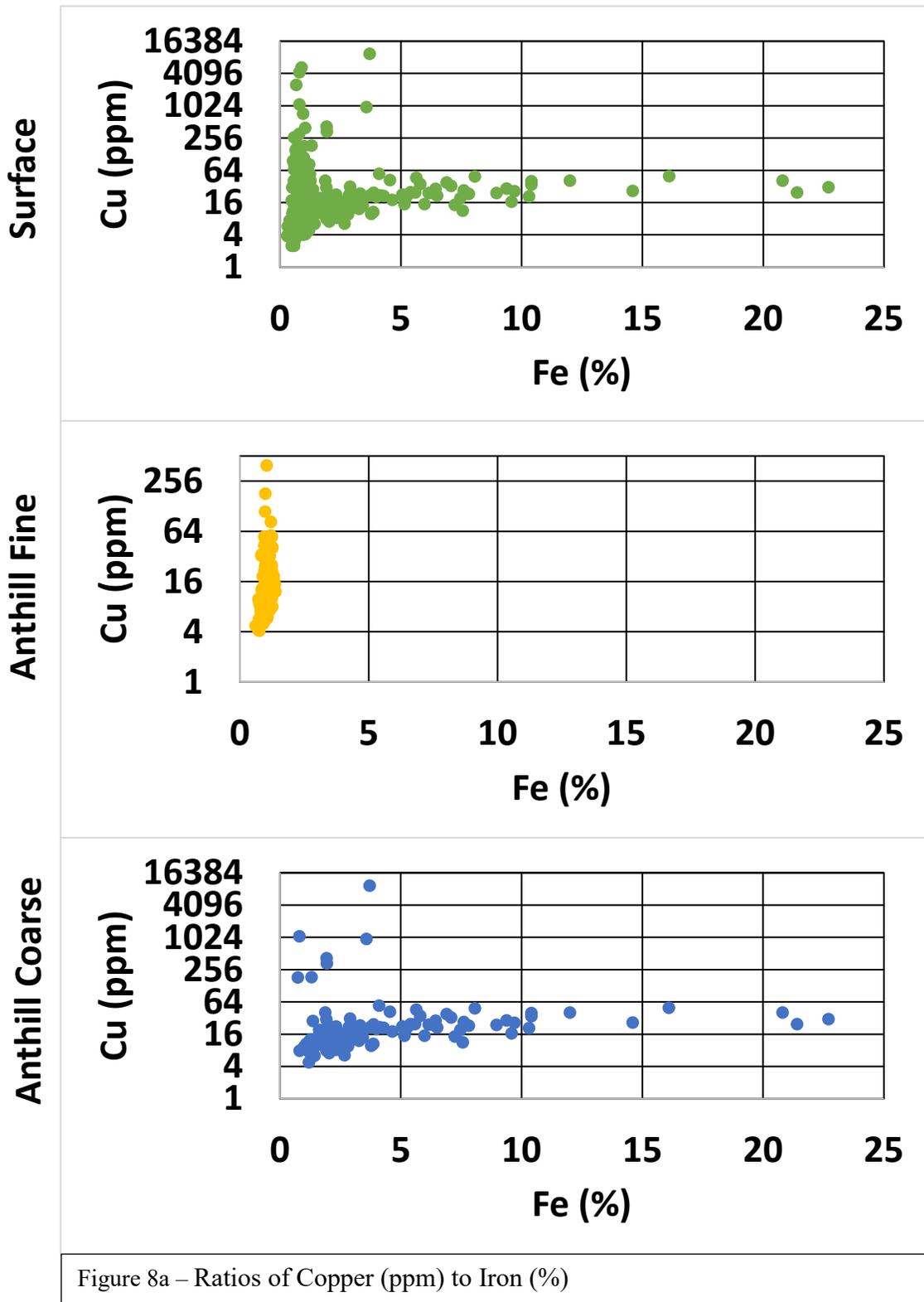
From the afore mentioned phase chronology of copper generation in this paper, the mineralization history doesn't include barium in its phases. Due to the observable barite cement in electron images, during its migration the solution must have carried copper ions. This is a proposed chronology on fluid migration and barite/copper mineralization after petroleum reduces the surrounding rock:

1st phase: Migration of barite and dolomite oxidized brines (short-chained carboxylic acid) carry copper ions (Jon Thorson, 2018, personal communication). The solution buffered with surrounding rock, and the solution concentrated and deposited hypogene copper (chalcocite).

2nd phase: More migration and buffered interactions with surrounding rocks caused fluid to precipitate barium. The barite cement became more stable, which caused the remainder of copper to exsolve out as supergene copper (chalcopyrite, malachite and azurite). Exposure and interaction with meteoric waters started to alter/ dissolve copper carbonates. Descending fluids concentrated between the zones as more supergene copper.

Barite cement raises the quandary not only because it shares a solid-solution series with lead, but about how it may affect in-situ recovery of copper. The proposed shallow injections of acids for leach recovery will

dissolve the copper, but it is not clear how the acids will interfere with the barite cements. This would be a solubility problem and future work might include finding out how barite reacts with pH and understanding the capillary pressures of the economic unit with mercury injection.
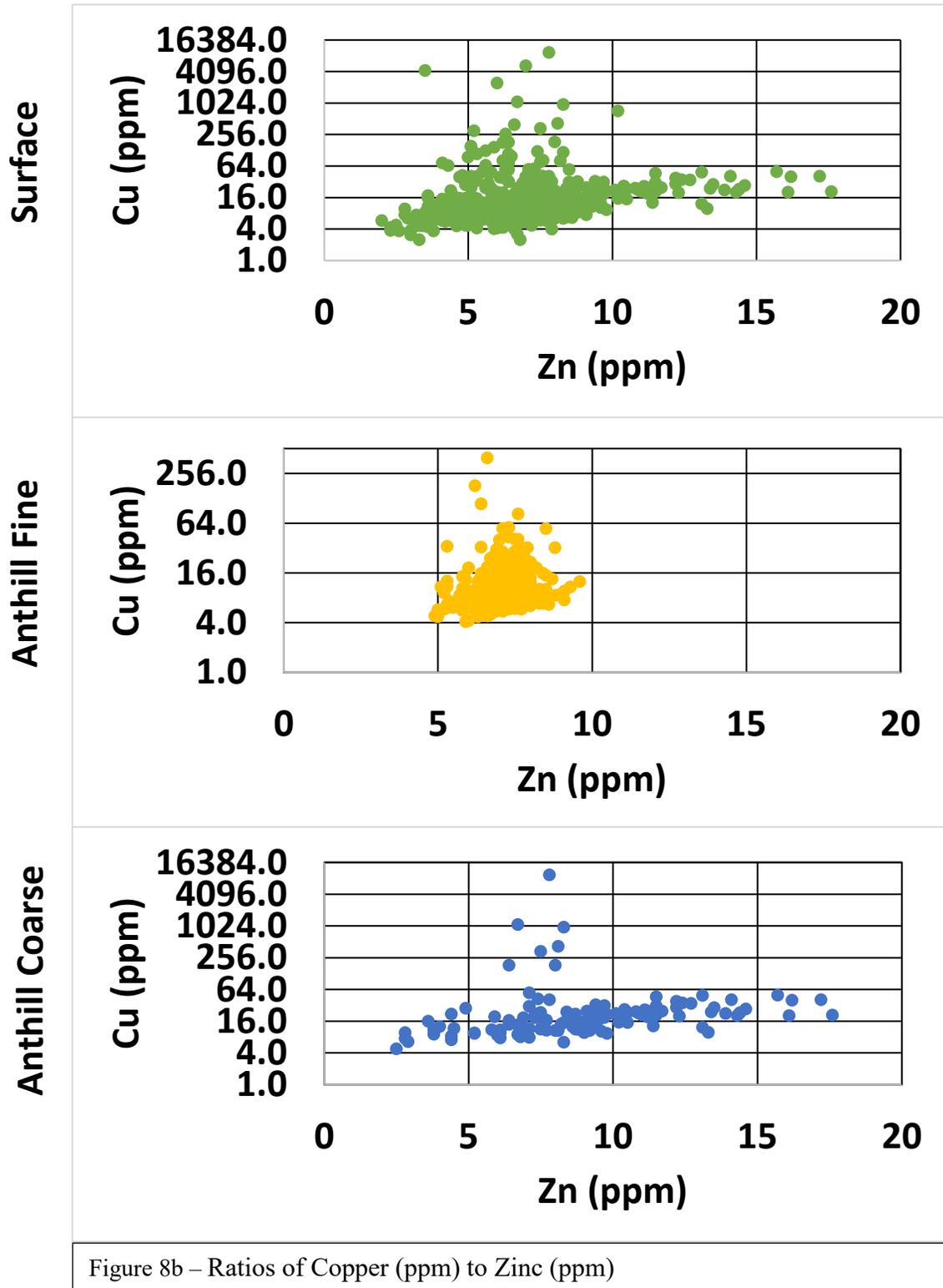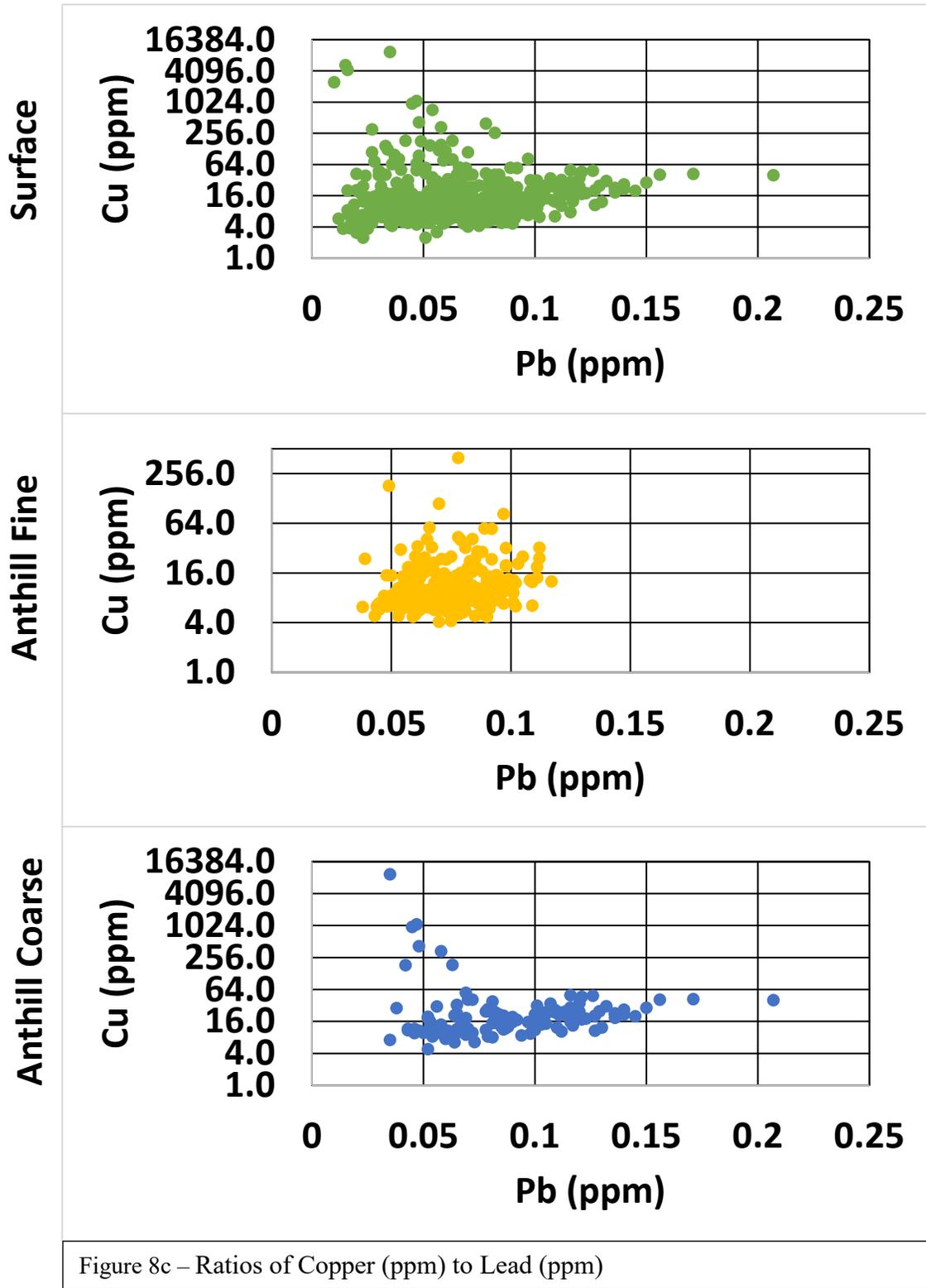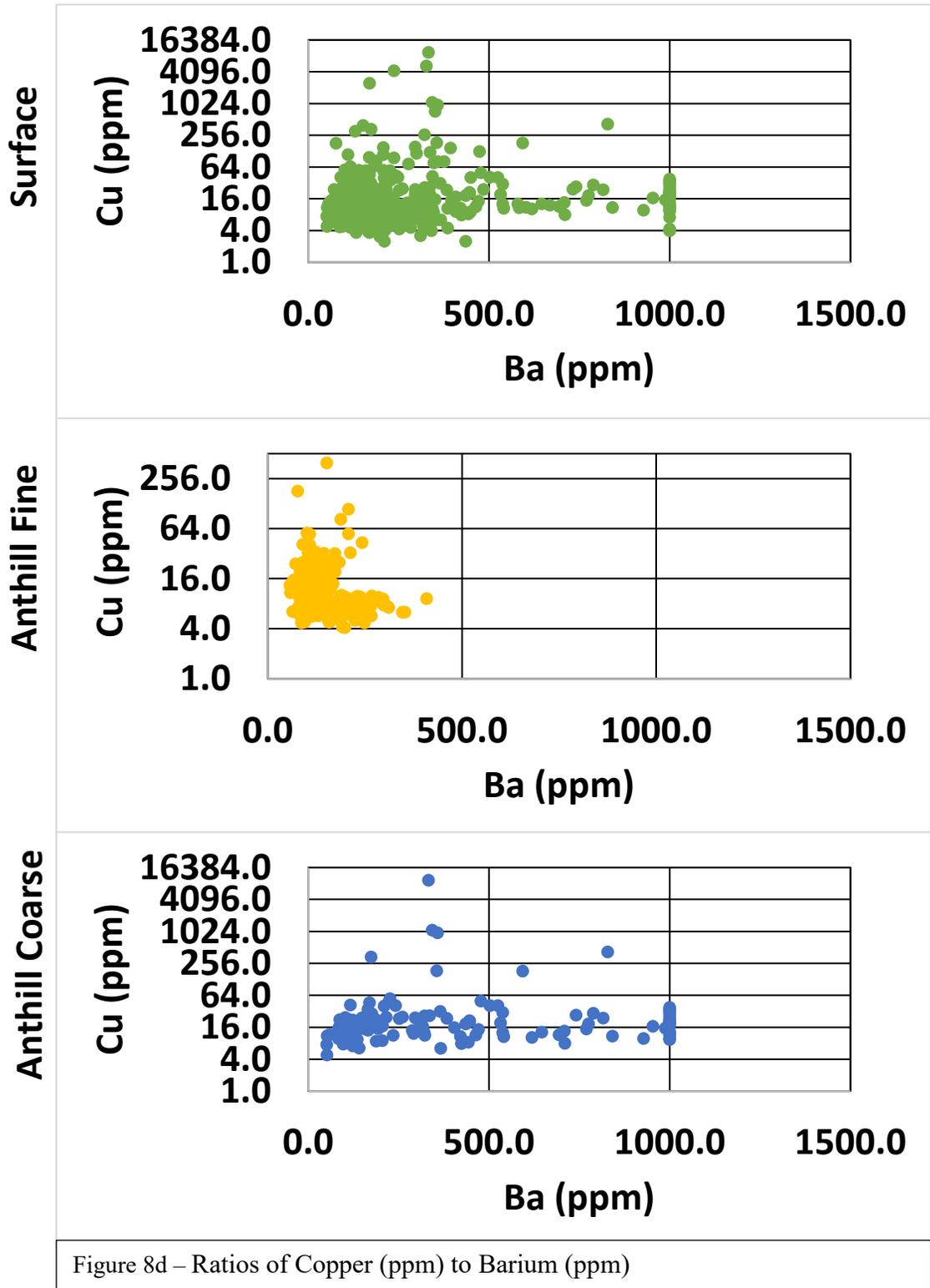

Figure 8a – Ratios of Copper (ppm) to Iron (%)

Figure 8b – Ratios of Copper (ppm) to Zinc (ppm)

Figure 8c – Ratios of Copper (ppm) to Lead (ppm)

Figure 8d – Ratios of Copper (ppm) to Barium (ppm)

References Cited

Adkins, A. R., Thorson P. T., and Geiger F., 2011, Integrated exploration techniques for sediment-hosted copper, lower Lisbon Valley, Utah, *in* Proceedings, Geological Society of Nevada Symposium, 2010: Reno Nevada, Great Basin Evolution and Metallogeny, p. 585-607.

Barbeau, D.L., 2003, A flexural model for the Paradox Basin: Implications for the tectonics of the Ancestral Rocky Mountains: Basin Research, v. 15, p. 97–115, doi: 10.1046/j.1365-2117.2003.00194.x.

Brooks, R. R., 1983, Biological methods of prospecting for minerals: Biological Methods of Prospecting for Minerals, J. Wiley, pp. 102–105. ISBN-13: 978-0471874003

Buffington, D. L. et. al., 2005, Lisbon Valley copper project, Lisbon Valley San Juan County, Utah: Technical Report Form 9434.00, Pincock, Allen & Holt and Constellation Copper Corporation

Fleshman, B. R., 2005, Lisbon Valley uranium project, Lisbon Valley San Juan County, Utah: Technical Report Form 43-101F1, BZU Minerals Ltd. and Fintry Enterprises Inc.

Hite, Robert J., 1960, Stratigraphy of the saline facies of the Paradox Member of the Hermosa Formation of southeastern Utah and southwestern Colorado: Four Corners Soc. Guidebook, 3rd Field Conf., p. 86-89.

Jacobs, M. B., and Kerr, P. F., 1965, Hydrothermal alteration along Lisbon Valley fault zone, San Juan County, Utah: Geological Society of America Bulletin, v. 76, no. 4, p. 423-440. doi: 10.1130/0016-7606(1965)76[423: HAATLV]2.0.CO;2

Kelley, V. C., 1955, Regional tectonics of the Colorado Plateau and relationships to the origin and Distribution of Uranium: Univ. New Mexico Press, Albuquerque, p.120.

Leary, R. J., Umhoefer, P., Smith, M. E., and Riggs, N., 2017, A three-sided orogen; a new tectonic model for ancestral Rocky Mountain uplift and basin development: Geology (Boulder), v. 45, no. 8, p. 735-738. doi: 10.1130/G39041.1

Robb, Laurence, 2017, Hydrothermal ore-forming processes: Introduction to Ore-forming Processes: Blackwell Science Ltd and Publishing, Oxford, United Kingdom, p. 197-202

Acknowledgements

Appendices 1: SEM Spectra (25 sample points) Y-axis shows the counts (number of X-rays received and processed by the detector) and the X-axis shows the energy level of those counts in kiloelectron volts (keV)